REPORT DOCUMENTATION PAGE

Form Approved OMB NO. 0704-0188

1. REPORT DATE (DD-MM-YYYY)	2. REPORT TYPE	3. DATES COVERED (From - To)
	Technical Report	-

4. TITLE AND SUBTITLE
Real-Time Distributed Implementation of Interference Alignment with Analog Feedback

5a. CONTRACT NUMBER
W911NF-10-1-0420

5b. GRANT NUMBER

5c. PROGRAM ELEMENT NUMBER
611102

6. AUTHORS
Seogoo Lee, Andreas Gerstlauer, Robert W. Heath Jr.

5d. PROJECT NUMBER

5e. TASK NUMBER

5f. WORK UNIT NUMBER

7. PERFORMING ORGANIZATION NAMES AND ADDRESSES
University of Texas at Austin
101 East 27th Street
Suite 5.300
Austin, TX 78712 -1539

8. PERFORMING ORGANIZATION REPORT NUMBER

9. SPONSORING/MONITORING AGENCY NAME(S) AND ADDRESS(ES)
U.S. Army Research Office
P.O. Box 12211
Research Triangle Park, NC 27709-2211

10. SPONSOR/MONITOR'S ACRONYM(S)
ARO

11. SPONSOR/MONITOR'S REPORT NUMBER(S)
58082-NS.13

12. DISTRIBUTION AVAILIBILITY STATEMENT
Approved for public release; distribution is unlimited.

13. SUPPLEMENTARY NOTES
The views, opinions and/or findings contained in this report are those of the author(s) and should not contrued as an official Department of the Army position, policy or decision, unless so designated by other documentation.

14. ABSTRACT
Interference alignment (IA) is known to achieve the maximum capacity for the interference channel. IA is a precoding technique to make interfering signals be aligned at receivers. The resulting sum rate is linearly scaled with the number of users. The performance of IA, however, depends on the practical issues

15. SUBJECT TERMS
interference,prototyping, wireless

16. SECURITY CLASSIFICATION OF:			17. LIMITATION OF ABSTRACT	15. NUMBER OF PAGES	19a. NAME OF RESPONSIBLE PERSON
a. REPORT	b. ABSTRACT	c. THIS PAGE			Robert Heath, Jr.
UU	UU	UU	UU		19b. TELEPHONE NUMBER 512-232-2014

Report Title

Real-Time Distributed Implementation of Interference Alignment with Analog Feedback

ABSTRACT

Interference alignment (IA) is known to achieve the maximum capacity for the interference channel. IA is a precoding technique to make interfering signals be aligned at receivers. The resulting sum rate is linearly scaled with the number of users. The performance of IA, however, depends on the practical issues such as the performance of synchronization, channel estimation and feedback. In this paper, a prototype is implemented for the IA system with three users. There have been IA prototypes in recent years, but the previous prototypes have not considered the distribution of the nodes in IA network. The nodes are physically distributed in our prototype not sharing their time and frequency references with any other, thus working independently, which enables the experimental study of IA under the most practical setup. For the distributed system, the over-the-air schemes for time and frequency synchronization and analog feedback are studied and implemented. According to the measurement from our prototype, it is shown that IA achieves the sum rate from the previous analysis on imperfect channel information. In addition, some other measurements are performed considering the accuracy of IA solution, synchronization of nodes, and CSI feedback. For the accuracy of IA solution, the performance of IA versus the number of iterations for an iterative IA method is measured. For synchronization accuracy, the performance with different residual frequency offset is measured. Finally, for the CSI feedback quality, analog feedback and scaler quantization-based limited feedback is first compared, and then the performance with Doppler frequency offset is also measured.

Real-Time Distributed Implementation of Interference Alignment with Analog Feedback

Seogoo Lee, *Student Member,* Andreas Gerstlauer, *Senior Member,* and Robert W. Heath Jr., *Fellow*

***Abstract*—Interference alignment (IA) is known to achieve the maximum capacity for the interference channel. IA is a precoding technique to make interfering signals be aligned at receivers. The resulting sum rate is linearly scaled with the number of users. The performance of IA, however, depends on the practical issues such as the performance of synchronization, channel estimation and feedback. In this paper, a prototype is implemented for the IA system with three users. There have been IA prototypes in recent years, but the previous prototypes have not considered the distribution of the nodes in IA network. The nodes are physically distributed in our prototype not sharing their time and frequency references with any other, thus working independently, which enables the experimental study of IA under the most practical setup. For the distributed system, the over-the-air schemes for time and frequency synchronization and analog feedback are studied and implemented. According to the measurement from our prototype, it is shown that IA achieves the sum rate from the previous analysis on imperfect channel information. In addition, some other measurements are performed considering the accuracy of IA solution, synchronization of nodes, and CSI feedback. For the accuracy of IA solution, the performance of IA versus the number of iterations for an iterative IA method is measured. For synchronization accuracy, the performance with different residual frequency offset is measured. Finally, for the CSI feedback quality, analog feedback and scaler quantization-based limited feedback is first compared, and then the performance with Doppler frequency offset is also measured.**

***Index Terms*—Interference alignment, prototyping, analog feedback.**

I. Introduction

Interference management plays a crux role in current wireless technologies since it allows the efficient use of limited time and frequency resources. Time division multiple access (TDMA) and frequency division multiple access (FDMA) have been used as simple interference management techniques in the past wireless systems. Due to the inherent nature of inefficiency in the spectrum usage, however, they cannot support the evolving wireless systems that require high spectral efficiency. This motivates the study for effective interference management methods using power control or precoding techniques that improve the spectrum efficiency significantly, especially when the multiple user pairs communicate concurrently using shared time and frequency.

The concept of interference alignment (IA) is first proposed for multiple input and multiple output (MIMO) X channel in [1]. The key idea of IA is to make the multiple interference streams be aligned at a receiver so that the dimensions for the subspace occupied by the interference streams are minimized while ensuring the independence of the desired streams. In [1], dirty paper coding (DPC) at transmitters and successive interference cancellation (SIC) at receivers are combined to achieve optimal multiplexing gain. As a result, two interfering streams are aligned in one antenna subspace and the desired streams are received without interference in the other antenna subspaces. In [2], it is shown that the same degree of freedom (DOF) can be achieved also for the MIMO X channel with zero forcing linear technique instead of non-linear DPC and SIC.

IA has also extended to K-user interference channel in [3]. The separation of the desired streams and the interference streams is done by linear precoding at transmitters and decoding at receivers. For K-user system, the DOF can be linearly increased with the number of users. This is the main difference of IA from the other orthogonal multiple access schemes where the DOF is fixed regardless of the number of users. The subspace for IA can be time, frequency or antenna subspace. It is shown in [3], however, that to use multiple antennas is the most efficient way to form the required dimensions for IA. In [4], [5], the feasibility conditions on the number of antennas for IA is studied.

The core task of IA is to find precoding vectors. Several schemes exist to find the IA precoding vectors : the closed form method in [3] and the iterative methods in [6] and [7]. The closed form solution in [3] is simple, but only exists for three users, while the iterative methods can be used with any number of users. In [6], by assuming feedforward and feedback channels' reciprocity in time division dumplex (TDD) system, the iteration is done between the transmitter side and the receiver side, and IA is used for both the feedforward data and the feedback data. Two optimization problems are also suggested in [6] for the iterative methods : one to minimize total interference leakage, and the other to maximize signal to interference and noise ratio (SINR). The key in [6] is that the algorithms do not need channel state information (CSI) feedback, and can be done in a fully distributed manner due to the channel reciprocity. In [7], the iteration is performed at either the transmitter side or the receiver side, not between them. The base algorithm in [7] is the same with the algorithm that minimizes total leakage in [6], but there is no assumption for the channel reciprocity and the algorithm in [7] requires CSI feedback.

Although IA provides a promising capacity gain in the interference network, it depends strongly on the assumptions such as perfect synchronization and CSI at transmitter (CSIT), which are infeasible in practice. IA considering these practical issues are studied with both analytical and experimental approaches.

For the analytical approaches, the CSI feedback quality is

studied when limited feedback [8] or analog feedback [9] is used. Furthermore, IA's performance in imperfect channel information is also studied in [10]. In [10], it is assumed that the CSI feedback is given with analog feedback, and IA's performance with imperfect feedback is analyzed with the CSI errors caused by the channel estimation error in feedforward channel, the channel estimation error in feedback channel, and the decoding error of CSI data in feedback channel.

Some work has studied the feasibility with the experimental approaches. In [11], [12], [13] and [14], IA prototypes are built and the performance of IA is measured and studied from them. In [11], the feasible setups for IA for wireless LAN system and the imperfect practical issues such as synchronization errors are studied. In [12], the wireless channel is measured from the authors' prototype, and the sum rate is calculated from it mainly showing that the gain in sum rate achieves under the measured channel. In [13], [14], the CSI is measured at the receivers, precoding vectors are obtained with the CSI, and the sum rate is calculated from over-the-air precoded transmission.

The main contribution of this paper is the first implementation and measurement of real-time distributed IA system. Though there have been the experimental studies of IA in literature, none has considered the practical issues when the nodes of IA are physically distributed, and consequently the system goes with overhead and accuracy loss in sharing CSI. Over-the-air time and frequency synchronization and feedback mechanisms are implemented to achieve this goal. From the prototype, the sum rate is measured showing that IA has a significant gain over the issues. Also, some other measurements are performed considering the accuracy of IA solution, synchronization and CSI feedback mainly showing the relationship between overhead and performance.

This paper is organized as follows : Section II briefly describes system model and background. Section III presents our approaches for distributed IA system. Section IV shows the implementation details and the results. Finally, Section V concludes this paper.

Throughout this paper, the following notations are used. K is the number of users in IA network, N_t and is the number of antennas at a transmitter and N_r is the number of antennas at a receiver. N_s is the number of the desired data streams for each user's transmitter and receiver pair. $\sup_n$ is the least upper bound of set n.

II. System model and background

Our system models K-user interference channel. For the interference channel, there is one by one mapping of a transmitter and a receiver as the example with $N_s = 1$, $N_t = 2$ and $N_r = 2$ in Figure 1. Only the data streams from i-th transmitter is the desired streams to i-th receiver, and the streams from the other transmitters are the interfering streams. Each of the transmitters and the receivers has N_t and N_r antennas respectively, and all nodes are separated. Assuming narrowband block fading channel, the received signal $\mathbf{y}_k$ at receiver node k is given by,

$$\mathbf{y}_k = \mathbf{H}_{k,k}\mathbf{F}_k\mathbf{d}_k + \sum_{m\neq k}\mathbf{H}_{k,m}\mathbf{F}_m\mathbf{d}_m + \mathbf{n}_k \quad (1)$$

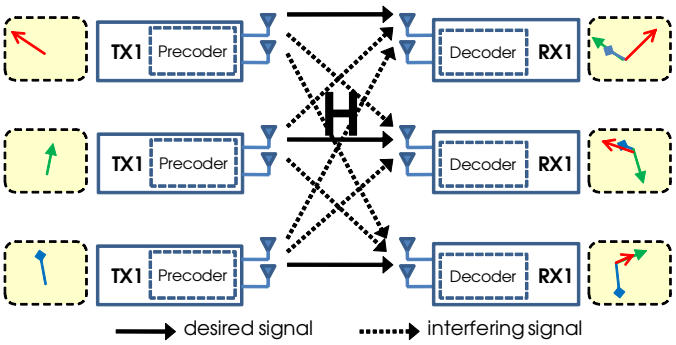

Fig. 1. Block diagram of 2×2 MIMO 3 user system.

where $\mathbf{H}_{k,m}$ is $N_r \times N_t$ channel matrix between k-th transmitter and m-th receiver, $\mathbf{F}_k$ is $N_r \times N_s$ precoding vector, $\mathbf{d}_k$ is $N_s \times 1$ data stream for k-th user pair, and $\mathbf{n}_k$ is additive white Gaussian noise (AWGN) at receiver k. The elements in $\mathbf{H}_{k,m}$ is independent identically distributed (i.i.d.).

A. Interference alignment

IA is a linear precoding technique that maximizes multiplexing gain for the interference channel. By precoding at the transmitters, multiple interfering streams are aligned in the same subspaces at the receiver side, and the interfering streams' subspaces are independent of the desired streams' subspaces. With a zero forcing decoder at the receivers, the received signal becomes,

$$\hat{y_k} = \mathbf{W}_k^H\mathbf{H}_{k,k}\mathbf{F}_k\mathbf{d}_k + \sum_{m\neq k}\mathbf{W}_k^H\mathbf{H}_{k,m}\mathbf{F}_m\mathbf{d}_m + \mathbf{W}_k^H\mathbf{n}_k. \quad (2)$$

Here, $\mathbf{W}_k$ is $N_r \times N_s$ decoding vector at receiver k. The first term from (2) is the desired signal after decoding which has the rank of N_s while the second term is the interference and becomes zero.

$$\mathbf{W}_k^H\mathbf{H}_{k,m}\mathbf{F}_m = 0 \quad (3)$$

$$\mathbf{W}_k^H\mathbf{H}_{k,k}\mathbf{F}_k \geq c > 0 \quad (4)$$

The sum rate R_{sum} of IA system is defined by the ratio of the desired signal's power and the sum of interference leakage power and noise power as follows.

$$R_{sum} = \sum_{k=1}^{K} log_2(I + \frac{\|\mathbf{W}_k^H\mathbf{H}_{k,k}\mathbf{F}_k\|^2}{\sum_{m\neq k}\|\mathbf{W}_k^H\mathbf{H}_{k,m}\mathbf{F}_m\|^2 + \sigma_k^2}) \quad (5)$$

With infinite symbol extension in time or frequency domain, the DOF of IA is $K/2$ as,

$$\sup_n \frac{(n+1)^N + (K-1)n^N}{(n+1)^N + n^N} = \frac{K}{2} \quad (6)$$

where n is any positive integer and $N = (K-1)(K-2)-1$.

With multiple antennas, the DOF depends on the antenna configuration and

$$\min(N_t, N_r)\frac{R}{R+1}K. \tag{7}$$

Here, $R = \frac{max(N_t,N_r)}{min(N_t,N_r)}$.

There are two different approaches to find the solution for linear IA precoding vectors : the closed form solution [3] and the iterative methods [6] and [7]. The closed form solution is available only for three user system. For the closed form solution, the interfering streams from transmitter two and transmitter three should be aligned at receiver one as follows.

$$\mathbf{H}_{1,2}\mathbf{F}_2 = \mathbf{H}_{1,3}\mathbf{F}_3 \tag{8}$$

Then, $\mathbf{F}_3$ can be obtained as

$$\mathbf{F}_3 = \mathbf{H}_{1,3}^{-1}\mathbf{H}_{1,2}\mathbf{F}_2. \tag{9}$$

Similarly at receiver three, interfering streams from transmitter one and transmitter two should be aligned, and $\mathbf{F}_1$ is

$$\mathbf{F}_1 = \mathbf{H}_{3,1}^{-1}\mathbf{H}_{3,2}\mathbf{F}_2. \tag{10}$$

At receiver two, interfering streams from transmitter one and transmitter three should be aligned, and together with (9) and (10), $\mathbf{F}_2$ is any eigenvector of $\mathbf{E}$, where $\mathbf{E}$ is,

$$\mathbf{E} = \mathbf{H}_{3,2}^{-1}\mathbf{H}_{3,1}\mathbf{H}_{2,1}^{-1}\mathbf{H}_{2,3}\mathbf{H}_{1,3}^{-1}\mathbf{H}_{1,2}. \tag{11}$$

The iterative methods find IA solution by numerical approaches. The iteration happens between transmitter side and receiver side by utilizing the channel reciprocity [6], or at either transmitter side or receiver side [7]. There are two optimization problems in [6] : minimizing interference leakage and maximizing SINR. The optimization problem to minimize interference leakage is also used in [7] as follows.

$$\max_{\substack{\mathbf{F}_m^*\mathbf{F}_m=\mathbf{I}_{N_s} \\ \mathbf{W}_k^*\mathbf{W}_k=\mathbf{I}_{N_k-N_s}}} \sum_{k=1}^{K}\sum_{\substack{m=1 \\ m\neq k}} \|\mathbf{H}_{k,m}\mathbf{F}_m - \mathbf{W}_k\mathbf{W}_k^*\mathbf{H}_{k,m}\mathbf{F}_m\|_{\mathbf{F}}^2 \tag{12}$$

The following procedure is performed to solve the above problem.

1) Choose the set of $\mathbf{F}_m$ randomly.
2) Choose the columns of $\mathbf{W}_k$ to be the $N_k - N_s$ dominant eigenvectors of $\sum_{m\neq k}\mathbf{H}_{k,m}\mathbf{F}_m\mathbf{F}_m^*\mathbf{H}_{k,m}^*$ $\forall k$.
3) Choose the columns of $\mathbf{F}_m$ to be the N_s least dominant eigenvectors of $\sum_{m\neq k}\mathbf{H}_{k,m}^*(\mathbf{I}_{N_k} - \mathbf{W}_k\mathbf{W}_k^*)\mathbf{H}_{k,m}$ $\forall m$.
4) Repeat steps 2) and 3) until convergence.

Both the precoding vector set $\{\mathbf{F}_m\}$ and the decoding vector set $\{\mathbf{W}_k\}$ are obtained from the above procedure. The convergence is guaranteed, but the cost function (12) is not a convex function, so the algorithm can fall into local minimums. Different from the closed form solution, the iterative methods can be used for any number of users in IA system, and even can be used for distributed IA system without a dedicated feedback channel if the system uses TDD by utilizing the reciprocity of wireless channel. A heavy computational complexity, however, is required for the iterative methods because of the eigenvector calculation at every iteration.

For the decoding vectors at the receivers, the minimum mean squared error (MMSE) decoding vector is presented in [15]. The decoding vector $\mathbf{W}_k$ is

$$\mathbf{W}_k = (\sum_{k=1}^{K}\mathbf{H}_{k,m}\mathbf{F}_m\mathbf{F}_m^*\mathbf{H}_{k,m}^* + \sigma^2\mathbf{I})^{-1}\mathbf{H}_{k,k}\mathbf{F}_k \tag{13}$$

where σ^2 is noise variance.

B. Synchronization

The above basic analysis of IA assumes perfect synchronization and perfect CSI measurement and feedback, which are not feasible in real world. The requirement for time and frequency synchronization for IA is studied in [11]. It is known from [11] that the phase offsets caused by time and frequency synchronization errors is not a problem for IA. It is because the phase error in synchronization does not affect the antenna subspaces where IA works. Besides this requirement in synchronization, a protocol for over-the-air nodes' synchronization is required for the distributed system.

There are two types of synchronization for the distributed IA system : synchronization among transmitters and synchronization between the transmitter side and the receiver side. Once the former is achieved, then the latter becomes a point to point synchronization that is well studied in literature. Thus, the main concern on synchronization is the synchronization among transmitters.

For our interference channel model, all the transmitters use the same time and frequency resources to send their own streams, so the multiple streams are overlapped at the receivers. If the transmitters are asynchronous, then the receivers have to estimate and compensate different time and frequency offsets for each of the transmitted streams, and it is an expensive task for the receivers as an example of asynchronous multiuser MIMO system in [16]. Otherwise, if the transmitters are globally synchronized, the receivers need to estimate and compensate only the global time and frequency offsets for all the overlapped streams, and it has lower synchronization overhead than the case of the asynchronous transmitters.

For the transmitter synchronization, master-slave synchronization protocols have been proposed in [17], [18] and [19]. In [17], a precise symbol-level time synchronization protocol is introduced for wireless LAN systems, and in [18] a frequency synchronization method based on the time synchronization protocol in [17] is also presented. Figure 2(a) shows an example of the system that has different propagation delays between any two nodes. The protocol in [17] assumes different propagation delays, and one of the transmitters works as the master transmitter, and the others become the slave transmitters, and the goal is to align the transmitters in time and frequency so that the signals from all the transmitters arrive as close as possible in time and frequency at the receivers.

To acquire the propagation delays and the other internal delays in a node for this goal, each of the transmitters

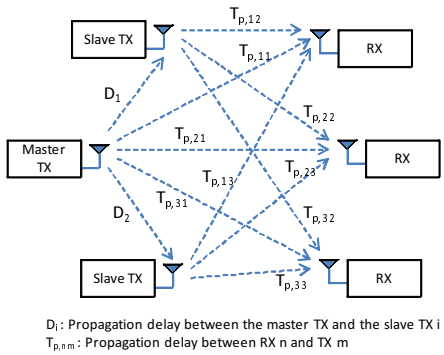

(a) System with different propagatin delays.

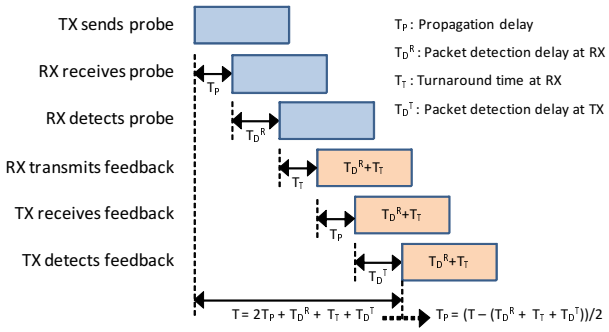

(b) Acquisition of one propagation delay.

Fig. 2. Over-the-air master-slave synchronization protocol.

periodically sends a probe to the others. Figure 2(b) shows the possible delay elements and the method how to obtain them. One transmitter sends the probe (This transmitter is denoted as 'TX' in Figure 2(b)), and then each of the other transmitters and the receivers (It is denoted as 'RX' in Figure 2(b)) senses the probe, measures the internal processing delay to detect the probe (T_D^R) and the turnaround delay from receiving mode to transmitting mode (T_T), informs the sum of those delays back to the transmitter that sends the probe. Then, the transmitter receives this feedback from each of the nodes, and measures the air propagation delays (T_P) with its internal detection time (T_D^T) and the delay information ($T_D^R + T_T$) given by the feedback node. The other transmitters perform the same task in turn.

When all the required delay information is obtained, the system is ready to work in synchronous manner. The master transmitter sends its training to the other transmitters, and each of the other transmitters adjusts the time with the previously measured delay information to send its own packet. After some time margin to this adjustment, all transmitters send their synchronized packets to the receivers. If multiple receivers exist in the system, however, it is impossible to make all receivers receive the transmitters' signals at the exactly same time. Instead, the transmitters adjust their packet transmission time so that the sum timing error at all the receivers to be minimized, e.g. all the signals are to be received within the cyclic prefix of orthogonal frequency division multiplexing (OFDM) system.

For frequency synchronization, the slave transmitters measure the frequency offset with the master's training, recover the offset before they send their data packet [18]. Along with the frequency offset, the phase offset between the master and the slaves are also considered in [18]. The phase offset caused by oscillator offset is inevitable, and it may affect the performance of wireless systems. To enable the slaves to measure the phase difference from the master, two identical trainings are sent from the master : one at the first transmission of the synchronization training and the other at actual data transmission. The slaves detect these two trainings and compare them to estimate phase offset between two. If the residual frequency offset is small, it can be assumed that there is only the constant phase offset between the master and a slave. The slaves also compensate the phase offset before their data transmission.

In [17], [18], TDD is assumed, but there is also a scheme that assumes frequency division multiplexing (FDD) and continuous transmission [19]. In [19], the master continuously sends its OFDM-based training to the slaves via a dedicated synchronization channel, and the phase rotation of OFDM subcarriers caused by time and frequency offset from the master is measured and compensated by the slaves before they send their own data stream.

C. CSI feedback

There are three major error types in CSI feedback : the error caused by AWGN, the limited feedback error and the delayed feedback error. The limited feedback error occurs by the quantization of the estimated CSI, and the delayed feedback error is by channel's time-varying property. IA with limited feedback is first analyzed in [8]. In [8], the CSI quantization error with Grassmannian codebook [20] is analyzed assuming perfect CSI measurment and feedback. According to its result, the DOF of $K/2$ for single input and single output IA system is achievable if the number of total feedback bits is larger than $K(L-1)logP_f$, where L is the number of multipaths in feedforward channel and P_f is the trasnmit power of CSI feedback.

The analog feedback with IA is presented in [9] to avoid the quantization error. In [9], the feedback channel estimation error by AWGN at feedback training and the feedback data error caused by AWGN at data symbols are considered. It is shown that the multiplexing gain of IA is preserved only with a constant sum rate loss when the transmitting power of feedback linearly relates to the transmitting power of feedforward. The upper bound of the constant sum rate loss ΔR_{sum} is given as the function of the length of the training for feedback channel estimation (τ_p), the length of the CSI feedback (τ_c), and the ratio of P_f and the transmit power P of feedfoward channel.

$$\Delta R_{sum}(\tau_p, \tau_c) \leq \sum_i d_i log_2(1+\frac{P}{P_f}c(\tau_p,\tau_c)(K-\frac{1}{d_i})). \quad (14)$$

Here, $c(\tau_p, \tau_c)$ is the value that depends on τ_p and τ_c, and if either τ_p or τ_c gets larger, $c(\tau_p, \tau_c)$ gets smaller showing that with more overhead in the feedback channel estimation training and feedback data, the sum rate loss ΔR_{sum} gets smaller. To maintain the multiplexing gain, P_f needs to

linearly scale with P, i.e. $P_f = \alpha P$. Otherwise, if P_f is not linear with P as $P_f = \alpha P^{\beta}$, there exists a loss in multiplexing gain according to β. A similar extended study also considering the feedforward channel estimation error is presented in [10].

III. System Realization

We are targeting 2×2 MIMO three user IA system as Figure 1. $N_t = N_r = 2$ for all user pairs, $N_s = 1$, and $K = 3$. OFDM is used for both feedforward and feedback channels. With this setup, two antenna subspaces are available for a user pair, and two interfering streams are aligned in one subspace at each receiver while the desired stream is received in the other subspace.

A. IA algorithms

Both the closed form solution and the iterative method in [7] are implemented in our prototype. For the closed form solution, the formulation in the previous section is directly implemented. For the iterative method, the heavy computation is required for the algorithm, and singular value decomposition (SVD) of 2×2 matrix is the main processing to find eigenvectors. To reduce the complexity of SVD and to be able to efficiently extend our implementation to more practical form, e.g. the embedded system with C++, the typical two step implementation scheme from [21] is used. The first stage is to decompose the target matrix into a real bidiagonal matrix. The second stage is to find the SVD of this bidiagonal matrix.

SVD can be written as follows.

$$\mathbf{B} = \mathbf{U}\mathbf{\Sigma}\mathbf{V}^H \tag{15}$$

Here, $\mathbf{B}$ is the vector to be decomposed, $\mathbf{U}$ and $\mathbf{V}$ are unitary matrices and $\mathbf{\Sigma}$ is a diagonal matrix with singular values. In this paper, we provide a brief summary of the algorithm, and the details are in [21]. In the first stage, we transform the target matrix as follows.

$$\mathbf{B} = \mathbf{U}_1 \begin{bmatrix} f & g \\ 0 & h \end{bmatrix} \mathbf{V}_1 = \mathbf{U}_1 \mathbf{D} \mathbf{V}_1. \tag{16}$$

Here, the elements of $\mathbf{D}$, f, g and h are real values.

In the second stage, the SVD of the real bidiagonal matrix $\mathbf{D}$ is found as

$$\mathbf{D} = \mathbf{U}_2 \mathbf{\Sigma} \mathbf{V}_2^T. \tag{17}$$

With (16) and (17), the final eigenvectors $\mathbf{U}$ and $\mathbf{V}$ become

$$\mathbf{U} = \mathbf{U}_1 \mathbf{U}_2 \tag{18}$$

$$\mathbf{V} = \mathbf{V}_1 \mathbf{V}_2. \tag{19}$$

B. Operation Scheduling

There are three main phases in IA operation scenario : training, feedback and data phases. Figure 3 summarizes the signals that are needed to be transmitted at each of the phases, and also shows the tasks that should be done during each of the phases at the transmitters and the receivers.

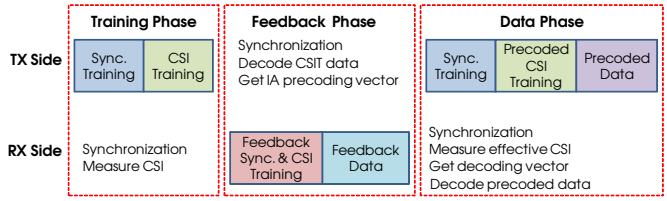

Fig. 3. Operation scenario for the prototype.

- **Training Phase** : This is mainly for CSI measurement at the receivers. The synchronization training is sent from the transmitters followed by the CSI training. The receivers first synchronize to the transmitters in time and frequency with the received synchronization training, and then measure CSI which should be given back to the transmitters at the feedback phase. Furthermore, the synchronization among the transmitters should be done at this phase. The details about the training structure and the transmitter synchronization is given in the following section.
- **Feedback Phase** : This phase is for CSI feedback. Each of the receivers makes a packet which is consisted of the synchronization training, the CSI training, and the CSI feedback data, and the packet is sent to the transmitters via over-the-air transmission. The packets are sent in time orthogonal manner. After receiving and decoding these packets, the transmitters calculate IA precoding vectors.
- **Data Phase** : This phase is for the precoded training and data transmission. The synchronization training, the precoded CSI training, and the precoded data are sent to the receivers in order. The receivers first synchronize to the transmitters, calculate the decoding vectors with the precoded CSI training, and decode the precoded data with them. Finally, the sum rate is calculated and the operation ends.

C. Over-the-air synchronization

The master-slave protocol is used for over-the-air transmitter synchronization in our prototype, but there are two differences from the algorithms in [17] and [18]. First of all, the phase synchronization in [18] is not required in our prototype since it does not affect IA performance. Also, time synchronization is simplified from [17]. The air propagation delays between nodes are assumed to be the same. This assumption is possible since the sample rate of our system is 1MHz, which means that the sample duration is long enough to avoid channel delay spread, and the nodes are not physically apart from each other by long distances to cause a symbol-level difference in the air propagation delays. With this assumption, there is no need to measure the air propagation delays. Then, the processing delay and the turn-around delay at both the transmitters and the receivers do not matter only if the following two requirements are guaranteed : 1) a symbol should be sent from transmitting antennas exactly at desired time at the transmitters, and 2) the exact time when a symbol arrives to receiving antennas is known at the receivers. These requirements are supported by our implementation hardware and software.

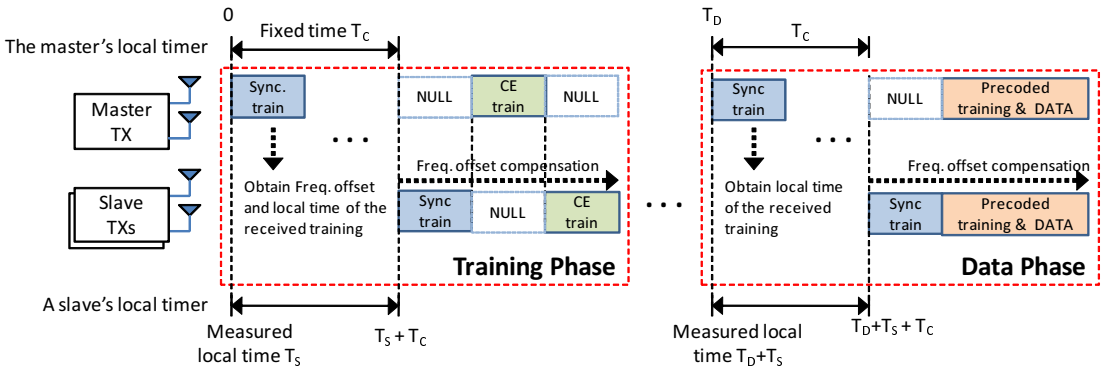

Fig. 4. Transmitter synchronization in our prototype.

Figure 4 illustrates our protocol. For our distributed system, it is assumed that each of the nodes are physically separated, and this means that every node works with its own time and frequency references not knowing the others' references. At the training phase which is the starting point of one turn of IA procedure, the synchronization is done in the following three steps,

- Step 1. The master transmitter first sends its training to the slave transmitters at time zero with its local timer. When each of the slaves receives and detects the training, it knows its local time $T_S^{[n]}$ when the first sample of the training is arrived at its antennas. Here, n is the slave index. The slaves also measure the frequency offset from the master's frequency with this training.
- Step 2. T_C is the waiting time for synchronized transmission, and it is known to all transmitters. The master and the slaves wait until their local time reaches T_C for the master, and $T_S^{[n]} + T_C$ for the slaves.
- Step 3. All the transmitters send their own training to the receivers immediately when their waiting time ends. Each of the slaves recovers the measured frequency offset from its own training before it is sent. The training and data are now synchronized in time and frequency.

The same operation is performed at the data phase since the time between the training phase and the data phase may not short enough for the slaves to maintain their previous synchronization. At the data phase, the starting time of the data phase, T_D, is only known to the master and it sends its training again to the slaves at that time. The slaves now detect it at time $T_S^{[n]} + T_D^{[n]}$, and all transmitters send the synchronization training and data after T_C time. Besides the transmitter synchronization, the receivers also need to synchronize to the transmitters. Each receiver synchronizes independently to the transmitters, and there is no coorperative synchronization among the receivers.

An auto-correlation method in [22] is used for synchronization at all nodes. Since the synchronization training has repeated patterns in time domain, the auto-correlation between two repeated patterns Γ_d becomes as follows :

$$\Gamma_d = \frac{|\Phi_d|^2}{P_d^2} = \frac{|\sum_{l=0}^{L_{rep}} y_k(d+l)y_k^*(d+l+G)|^2}{\sum_{l=0}^{L_{rep}} |y_k(d+l+G)^2|^2}. \quad (20)$$

Here, d is the current received sample, L_{rep} is the correlation length and G is the length of a pattern. The normalized auto-correlation Γ_d is the ratio of the auto-correlation Φ_d and the power P_d. The exact time synchronization point d_s is the d that maximizes Γ_d. The frequency offset is obtained from the arctangent value of Γ_{d_s}.

D. CSI Feedback

The main feedback scheme in this paper is analog feedback. Under the assumption of flat fading channel, receiver i measures

$$\mathbf{H}_{ij}, \quad j = 1, 2, 3. \quad (21)$$

Since each $\mathbf{H}_{ij}$ is 2×2 matrix, there are $K \times N_t \times N_r$ complex values for the measured CSI at each receiver. These values are mapped to N_{sc} subcarriers by $N_{sc} \times (K \times N_t \times N_r)$ mapping matrix, and the N_{sc} subcarriers form an OFDM symbol. As a result, each receiver has an OFDM symbol for analog feedback. The transmitters that receive the OFDM symbols apply the pseudo inverse of the mapping matrix to the received OFDM symbols, and find the CSI values. The transmit power which decides the difference in SNR between feedforward and feedback channel as in (14) is a design parameter.

For limited feedback as a competitor, the explicit feedback beamforming method from the beamforming specification of 802.11n wireless LAN is used [23]. With the quantization method, N_{gain} bits are used for the amplitude of CSI, and N_q bits are used to quantize each of real and imaginary values of the measured CSI. The integer amplitude index M_i in dB for receiver i's CSI feedback is

$$M_i = min\{2^{N_{gain}} - 1, \lfloor 20log_{10}(\frac{G_{ref}}{m_i}) \rfloor\}. \quad (22)$$

G_{ref} is the maximum gain reference, and m_i is the maximum absolute value among all the real and imaginary values

of $\mathbf{H}_{ij}, j = 1, 2, 3$. $\lfloor x \rfloor$ is the largest integer smaller than or equal to x. M_i index is given to the transmitters via feedback channel.

The real and imaginary values of $\mathbf{H}_{ij}$ are quantized and normalized to $\mathbf{H}^q_{scaled(ij)}$ which is consisted of N_q bits with two's compliment fixed point number representation as

$$Re(\mathbf{H}^q_{ij}) = round\left(\frac{Re(\mathbf{H}_{ij})}{M_i^{lin}}(2^{N_q-1}-1)\right) \quad (23)$$

$$Im(\mathbf{H}^q_{ij}) = round\left(\frac{Im(\mathbf{H}_{ij})}{M_i^{lin}}(2^{N_q-1}-1)\right). \quad (24)$$

Here, M_i^{lin} is the normalization factor given by $G_{ref}/10^{M_i/20}$. For each receiver, the total number of bits to be transmitted as CSI feedback is $N_{gain}+2\times N_q \times K \times N_t \times N_r$. These bits are mapped to QPSK modulation and OFDM subcarriers.

The transmitters that receive the CSI feedback first decode M_i and $\mathbf{H}_{received(ij)}$ by QPSK and OFDM decoding, then they find the CSI by

$$Re(\mathbf{H}_{received(ij)}) = \frac{Re(\mathbf{H}^q_{ij})}{10^{M_i/20}} \quad (25)$$

$$Im(\mathbf{H}_{received(ij)}) = \frac{Im(\mathbf{H}^q_{ij})}{10^{M_i/20}}. \quad (26)$$

$N_{gain} = 3$ and $N_q = 4, 5, 6$ and 8 for our implementation. G_{ref} is chosen to minimize the mean squared error (MSE) by quatization.

The quality of CSI feedback is also affected by Doppler frequency. To measure the performance of our system from Doppler effect, the Doppler effect model by memoryless Markov process is used as an example in [24]. Assuming the channel is Rayleigh block fading channel, the channel's time varying property by Doppler effect is modeled with Markov process as,

$$\mathbf{H}_{ij}[n] = \rho \mathbf{H}_{ij}[n-1] + e[n]. \quad (27)$$

Here, ρ is the channel correlation coefficient, and $e[n]$ is the channel error that has complex normal distribution. The constraint for ρ and $e[n]$ is $\rho^2 + e[n]^2 = 1$. If f_d is Doppler frequency and T_s is the symbol duration, ρ is given as $\rho = J_0(2\pi f_d T_s)$, where $J_0(x)$ is the 0-th order Bessel function of the first kind. It can be seen that if $\rho = 0$, the channels at n and $n-1$ are completely independent. On the other hand, if $\rho = 1$, the channel is perfectly known to the transmitters.

IV. Experiments and Results

TABLE I
OFDM PARAMETERS FOR THE PROTOTYPE.

FFT length	128
Cyclic Prefix Length	32
Number of null subcarriers	23
Number of data subcarriers	105

The system is designed to operate at 2.4 GHz, the bandwidth would ideally be large as 20 MHz, but it is lower as 1 MHz in our prototype because of hardware constraints. Both feedforward and feedback channel use the same frequency, and the system is a TDD system. OFDM is used for the training and data, and only the synchronization training is generated at time domain. The OFDM parameters are summarized in Table I.

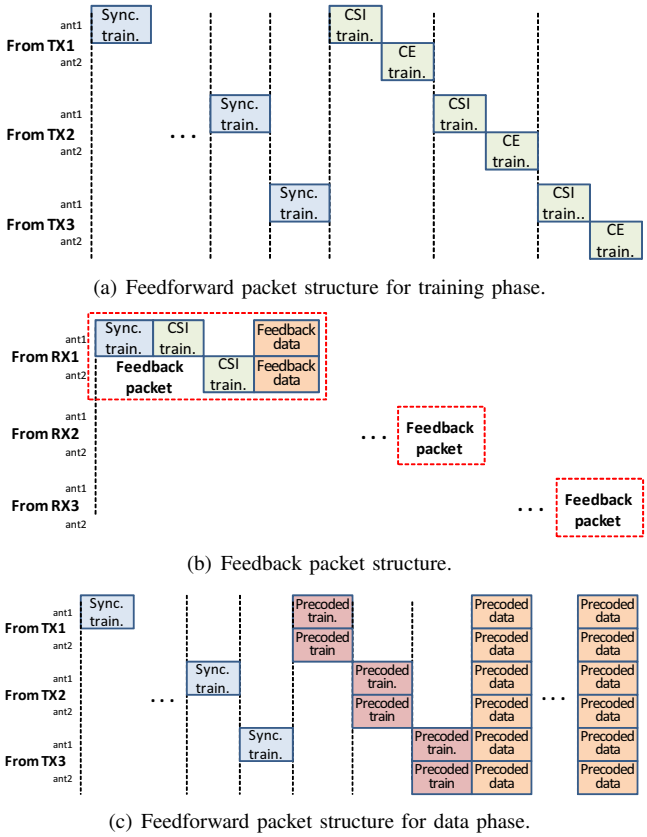

(a) Feedforward packet structure for training phase.

(b) Feedback packet structure.

(c) Feedforward packet structure for data phase.

Fig. 5. Packet structures.

A. Experiment setup

As described in the previous section, our system works in three phases : the training, the feedback and the data phases. For each of the phases, the packet structure is shown in Figure 5. In Figure 5, the packet structures for the training phase (Figure 5(a)), the feedback phase (Figure 5(b)), and the data phase (Figure 5(c)) are given. There are three types of trainings in our system:

- **Synchronization training** : The synchronization training is for the nodes' synchronization. It has two parts : short training for coarse time synchronization and long training for fine time and frequency synchronization. A length 17 Zadoff-Chu sequence is repeated five times as the short training, and a length 29 Zaduff-Chu sequence is repeated three times as the long training. The training has repeated patterns in time domain, and the synchronization is done by the auto-correlation method in (20).
- **CSI training** : The CSI training is for CSI measurement to be sent back to the transmitters for IA precoding vector calculation. One CSI training is an OFDM symbol, and it is sent from each of the transmitting antennas

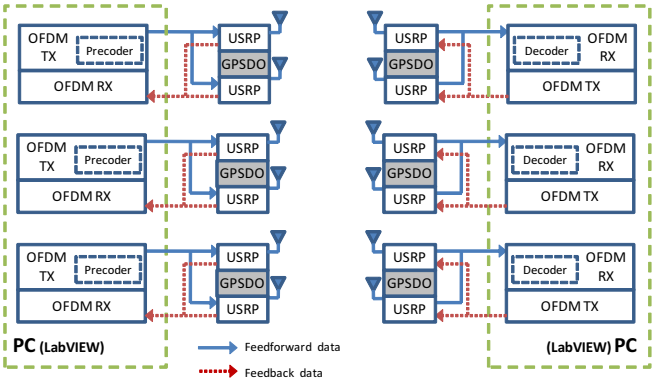

Fig. 6. Software and hardware configuration of the prototype.

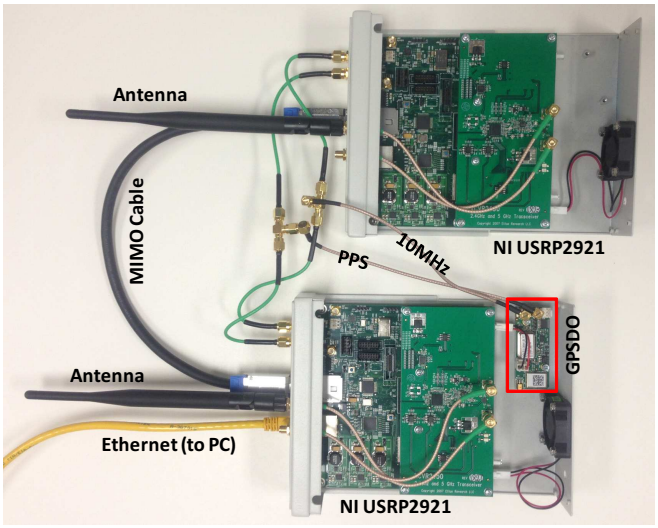

Fig. 7. Hardware configuration of one node.

in time orthogonal manner as in Figure 5(a). As such, six OFDM symbols are transmitted for our three user 2×2 MIMO system. The training does not experience precoding nor decoding. Thus, the receivers can find the pure condition of current wireless channel. With this training, each receiver measures 2×6 CSI matrix.

- **Precoded training** : The precoded training is sent at the data phase, and it experiences IA precoding at the transmitters, where each user in our three user system has one data stream that is mapped to two antennas via the precoding vector. It is used for the decoding vector calculation. Also, since this training is precoded in the same way with the precoded data, it is used to equalize the data symbols. The training is also an OFDM symbol, and it is sent from two transmitting antennas of a transmitter at a time. Each transmitters sends it in time orthogonal manner as in Figure 5(c).

B. Software and hardware

Figure 6 shows the hardware and software configuration of our prototype. The system uses two computers that are equipped with dual-core Intel Xeon 2.67 GHz processors and 12GB of memory. One computer is used to control the trasnmitters, and the other is for the receivers. National Instruments (NI) USRP-2921 [25] is used for analog to digital convertor (ADC) / digital to analog convertor (DAC) and radio frequency (RF) front-end. One USRP works as one antenna, so two USRPs are used for a node, and accordingly one computer controls six USRPs. A USRP can switch between transmitting mode and receiving mode, e.g. the USRPs for the transmitters work in transmitting mode for the training and data phases, but in receiving mode for the feedback phase. The computer and the USRPs are connected via TCP/IP connections. National Instruments (NI) LabVIEW which is a model-based digital signal processing implementation software [26] is used for our software defined radio (SDR) implementation. The control of USRPs is also done by LabVIEW's USRP driver. Though only one computer is used for all the transmitters, and similarly only one computer is used for all the receivers, the signal processing for each node is completely separated from each other not to violate the interference channel model, i.e. there are three parallel independent processing chains in LabVIEW on a computer.

Since our system is distributed system, each node should work with its own oscillator. The GPS disciplined oscillator (GPSDO) module that can be attached to USRP is used as the oscillator for a node [27]. The GPSDO is originally for the global synchronization to the GPS signal which is only available at outdoors. There is, however, no assumption of outdoor operation for IA system in general, so the GPSDOs are not used to synchronize to the global GPS signal. Instead, a GPSDO is used to provide time and frequency references only to a single node in our prototype. Though the GPSDOs are used, our distributed synchronization algorithm is designed assuming that each of the GPSDOs generates the independent time reference (pulse per second (PPS)) and frequency reference (10MHz) without being synchronized to the GPS signal since our prototype is tested in indoor environment where the global GPS signal is unavailable. The PPS and 10MHz are the required time and frequency references for the USRPs respectively. Six GPSDOs are used because there are six nodes in the system, and the time and frequency reference signals from a GPSDO are only shared between two USRPs which form a node's two antennas. Figure 7 shows the hardware configuration of a node in the prototype. The MIMO cable between the USRPs in Figure 7 is only used for the ethernet connection of two USRPs to a computer.

Figure 8 shows the schematic of distributed test environment. Both the transmitters and the receivers are physically separated to verify our system. To make the SNRs of the air links be similar as possible, the distances between any transmitter and any receiver are made to be the same as possible. Also, the AWGN generator which is used to scale the overall SNR of the system is located at the center of the nodes.

C. Results

In this paper, the sum rate of distributed IA with analog feedback is first presented. Then, more detailed measurements

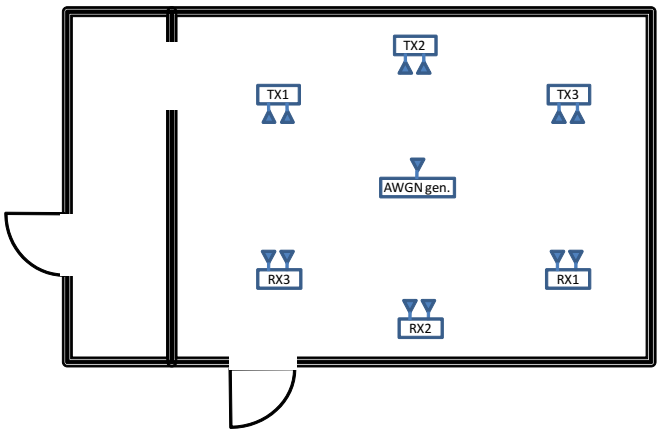

Fig. 8. Test environment of distributed nodes.

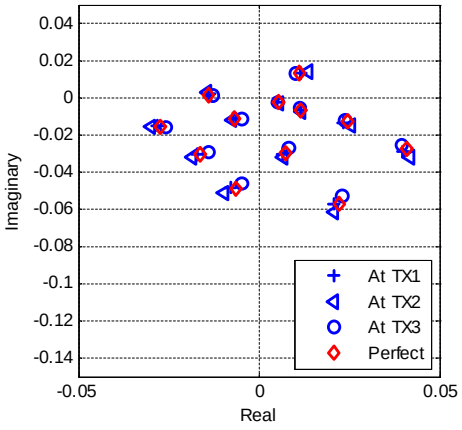

Fig. 9. An example constellation of analog feedback.

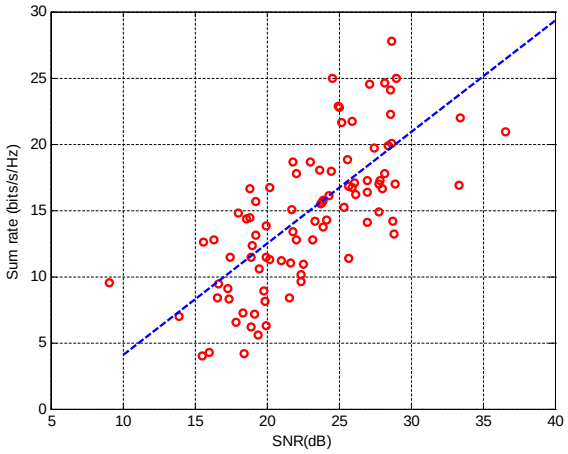

(a) Measured sum rate of distributed IA with analog feedback.

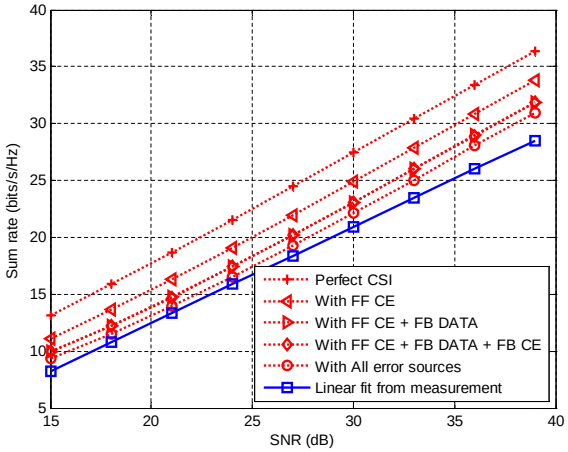

(b) Comparison of measured sum rate to simulated sum rate.

Fig. 10. IA performance with analog feedback

on the relationship between the accuracy of IA solution, residual frequency offset, and CSI feedback are also given. For all the results in this paper, the distributed nodes' synchronization protocol is applied.

To scale SNR of the system, Agilent E4438C vector signal generator is used [28]. A white Gaussian complex random data with 5,000 samples is generated from Matlab and uploaded to the signal generator, and the data is emitted repeatedly at 2.4GHz. By controlling RF gain from the signal generator, SNR can be changed, and it is measured at the receivers. SNR measurement is done by measuring the noise power from CSI training at frequency domain. After the channel estimation is done at frequency domain by FFT, this pre-channel estimation result is transformed into time domain samples by IFFT. Now the samples are channel's impulse responses, and the first few samples show the channel power and the following samples show noise power. By nulling the noise samples and performing FFT again, the noise free post-channel estimation result is obtained. The SNR is defined by the ratio of the signal power from noise free post-channel estimation result and the noise power from the difference between pre and post channel estimation results. The same transmit power is used both for feedforward and feedback channel, so the SNRs for both channels are the same.

Figure 9 shows an example of a packet's received CSI at the transmitters with analog feedback when the SNR is 30dB. Figure 9 has 12 constellation groups, and each group is an element of 2×6 $\{\mathbf{H}_{i1}, \mathbf{H}_{i2}, \mathbf{H}_{i3}\}$ channel matrix from i-th receiver. Four different points in a group show the received CSI at transmitter 1, 2, 3, and the perfect CSI.

The sum rate of our system is given in Figure 10. Each dot in the first subfigure is the measured instantaneous sum rate within SNR range from 15dB to 35dB and the solid line shows their linear fitting, and the second subfigure shows the comparison of the linear fitting to the simulation results. The simulation is performed under different setups : 1) perfect CSI estimation (CE) and feedback, 2) only with feedforward CE error, 3) with feedforward CE and feedback data errors, 4) with the errors in 3) and feedback CE error, and 5) with all the error sources : feedforward CE error, feedback data error, and feedback CE error, and feedforward precoded CE error. It is observed from Figure 10 that the multiplexing gain is maintained by analog feedback only with a constant sum rate degradation if the feedback transmit power is linear to the feedforward transmit power for CSI measurement as analyzed

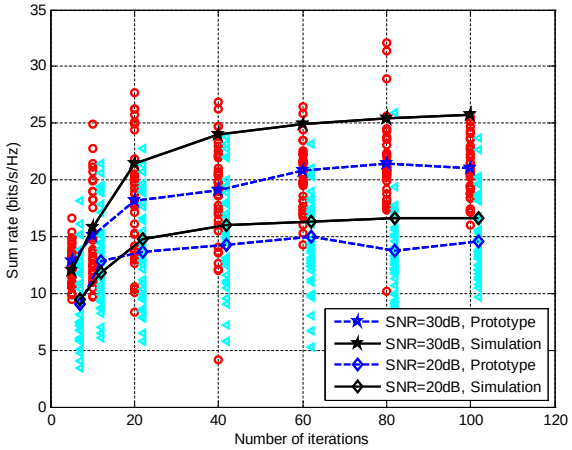

Fig. 11. Sum rate with iterative IA method.

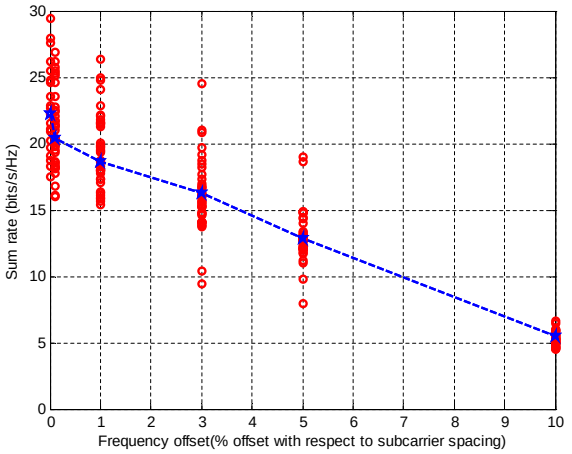

Fig. 12. IA performance with the residual frequency synchronization error

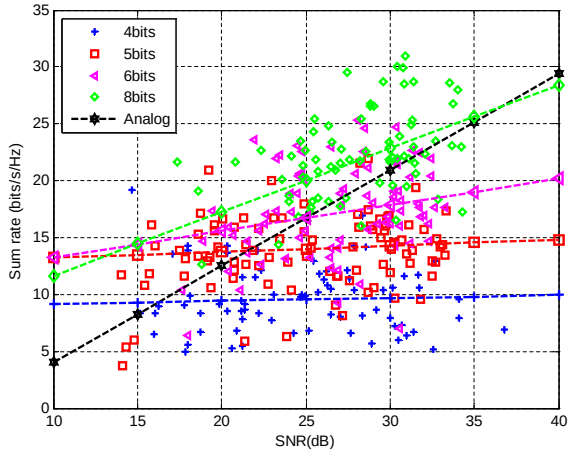

(a) Measured sum rate with limited feedback and analog feedback

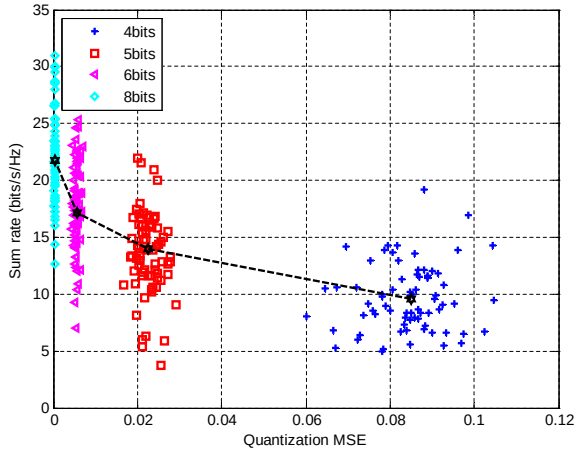

(b) Sum rate vs. MSE of limited feedback.

Fig. 13. IA performance with limited feedback

in [9]. This result is possible since the SNRs for feedforward channel and feedback channel are the same in our experiments.

To study the performance with imperfect IA solution, Figure 11 shows the sum rate versus the number of iterations for the iterative IA method. The iterative method from [7] is used, and the number of iterations is an important design parameter for the method. The mean sum rate at SNR = 30dB and SNR = 20dB are measured and compared to those from the simulation with the perfect CSI feedback. Though the sum rate from the prototype is smaller than that from the simulation because it is limited by CSI estimation and feedback, the number of iterations to achieve the sum rate is not reduced. This shows that the leakage from the imperfect IA solution is independent to the other error sources regardless of SNR of the system.

Figure 12 shows the IA performance with synchronization error. The time synchronization error of IA with OFDM does not affect the IA performance only if the timing synchronization is done only within cyclic prefix, and this requirement is not new to IA. Frequency synchronization, however, can not be perfect in the real systems, and there always remains the residual frequency offset after synchronization. It causes inter channel interference (ICI) which can not be recovered by IA, so it is added as an extra error source to the system. Furthermore, the ICI by the residual frequency offset affects all the CSI measurement and feedback steps which are listed in Figure 10. In Figure 12, the sum rate is plotted with different % frequency offsets with respect to the subcarrier spacing. The same frequency offset is added to the air links between the master transmitter and the slave transmitters, and to the connection between the transmitters and the receivers. The SNR is 30dB.

The analog feedback is also compared to limited feedback. For limited feedback, the uncompressed explicit scalar quantization in 802.11n specification [23] is used as described in the previous section. $N_q = 4, 5, 6$ and 8 are applied for the evaluation. It is observed from Figure 13(a) that the slope of sum rate increases as more bits are allocated, i.e. as feedback overhead is increased, which means more bits are needed as feedback as SNR gets high to get the multiplexing gain of IA. Figure 13(b) shows the sum rate against MSE of limited feedback. The fitting line is the linear connection of the means of the sum rates with different N_q. The results

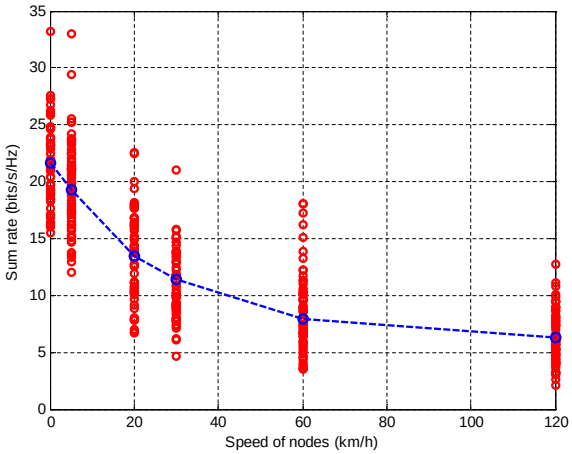

Fig. 14. IA performance with Doppler effect

in Figure 13 gives us some interesting observations. First of all, the multiplexing gain of quantization-based feedback increases with increasing number of N_q, which corresponds to the previous analysis in [8]. Furthermore, compared to the quantization-based feedback, analog feedback has higher sum rate performance at high SNR region than the quantization-based feedback. This is because the MSE of analog feedback is reduced with increasing feedback SNR, but the MSE of quantization-based feedback is fixed regardless of SNR if it is assumed that there is no bit error for quantization-based feedback.

The delay in CSI feedback also causes multiplexing gain degradation of IA. Figure 14 presents the sum rate measurement result versus the speed of nodes at 30dB SNR. The measured CSI is modified with the ρ and e from Markov process when the speed of node is given. The modified CSI is transmitted to the transmitter via analog feedback. The sample duration $T_s = 1ms$ is assumed. From Figure 14, it is obvious that IA is very sensitive to delayed feedback loosing most of sum rate gain at lower speed than 5 km/h.

V. Conclusion and Future Work

The prototype of the three user IA system with 2×2 antenna configuration for each user is implemented. With the prototype, the performance of IA with the practical issues is studied, and the interesting measurement results about feedback quality are first presented. Our IA system targets interference channel, so the nodes are assumed to be physically separated and to work independently without coorperation following the basic assumption of interference channel. It is achieved by developing over-the-air time and frequency synchronization protocol and feedback methods. The synchronization requirement of IA is studied, and the over-the-air master/slave synchronization method is developed. Analog feedback is implemented as the over-the-air feedback method, and the performance of IA with analog feedback in real world is verified from our prototype. The performance of IA with imperfect IA solution, synchronization and CSI feedback is also studied providing us the chances for design space exploration of IA's design parameters. Finally, the sum rate degradation according to mobility is measured showing a critical limitation of IA.

To move forward to enable IA in the practical applications, the achievable performance of IA with the hardware constraints in the real world such as the limited and heterogeneous computing capability of IA network as well as the limited energy supply of portable devices needs to be studied, and it remains as our future work.

Acknowledgment

The authors would like to thank Erik Luther of National Instruments, and Omar El Ayach of Qualcomm for their help and support in making this work possible.

References

[1] M.A. Maddah-Ali, A.S. Motahari and A.K. Khandani, "Signaling over MIMO Multi-Base Systems: Combination of Multi-Access and Broadcast Schemes," *IEEE International Symposium on Information Theory*, pp.2104-2108, July, 2006.

[2] S.A. Jafar, S. Shamai, "Degrees of Freedom Region of the MIMO X Channel," *IEEE Transactions on Information Theory*, vol. 54, no. 1, pp. 151-170, January 2008.

[3] V.R. Cadambe and S.A. Jafar, "Interference alignment and spatial degrees of freedom for the k user interference channel," *IEEE International Conference on Communications 2008*, pp. 971-975, May 2008.

[4] C.M. Yetis, T. Gou, S.A. Jafar and A.H. Kayran, "Feasibility Conditions for Interference Alignment," *Proceedings of IEEE GLOBECOM 2009*, December 2009.

[5] N. Lee, D. Park, and Y. Kim, "Degrees of freedom on K-user MIMO interference channel with constant channel coefficients for downlink communications," *Processings of IEEE GLOBECOM 2009*, December 2009.

[6] K. Gomadam, V.R. Cadambe and S.A. Jafar, "A Distributed Numerical Approach to Interference Alignment and Applications to Wireless Interference Networks," *IEEE Transactions on Information Theory*, vol. 57, no. 6, pp. 3309-3322, June 2011.

[7] S. W. Peters and R. W. Heath, Jr., "Interference Alignment via Alternating Minimization," *IEEE International Conference on Acoustics, Speech and Signal Processing (ICASSP) 2009*, pp. 2445-2448, April 2009.

[8] H. Bolcskei and I. Thukral, "Interference Alignment with Limited Feedback," *IEEE Int. Symp. Inf. Theory*, pp. 1759-1763, July 2009.

[9] O. E. Ayach and R. W. Heath Jr., "Interference Alignment with Analog Channel State Feedback," *IEEE Transactions on Wireless Communications*, vol. 11, no. 2, pp. 626-636, February 2012.

[10] O. El Ayach, A. Lozano and R.W. Heath, Jr., "On the Overhead of Interference Alignment: Training, Feedback, and Cooperation," *IEEE Transactions of Wireless Communications*, vol. 11, no. 11, pp. 4192-4203, November, 2012.

[11] S. Gollakota, S. D. Perli, and D. Katabi, "Interference alignment and cancellation," *Proceedings of the ACM SIGCOMM 2009*, pp. 159170, August 2009.

[12] O. E. Ayach, S.W. Peters, and R.W. Heath Jr., "The feasibility of interference alignment over measured MIMO-OFDM channels," *IEEE Transactions on Vehicular Technology*, pp. 43094321, 2010.

[13] O. Gonzalez, D. Ramirez, I. Santamaria, J. A. Garcia-Naya, and L. Castedo, "Experimental validation of Interference Alignment techniques using a multiuser MIMO testbed," *IEEE International ITG Workshop on Smart Antennas*, pp. 18, February 2011.

[14] J. W. Massey, J. Starr, S. Lee, D. Lee, A. Gerstlauer, and R. W. Heath Jr., "Implementation of a Real-Time Wireless Interference Alignment Network," *Asilomar Conference on Signals, Systems and Computers*, November 2012.

[15] S. Peters, R.W. Heath Jr., "Cooperative Algorithms for MIMO Interference Channels," *IEEE Transactions on Vehicular Technology*, vol. 60, no. 1, pp. 206-218, January 2011.

[16] T. Tang and R. W. Heath, Jr., "A Space-Time Receiver with Joint Synchronization and Interference Cancellation in Asynchronous MIMO-OFDM Systems," *IEEE Transactions on Vehicular Technology*, vol. 57, no. 5, pp. 2991-3005, September 2008.

[17] H. S. Rahul, H. Hassanieh and D. Katabi, "SourceSync: a distributed wireless architecture for exploiting sender diversity," *Proceedings of the ACM SIGCOMM 2010*, pp. 171-182, Aug. 2010.
[18] H. S. Rahul, S. Kumar and D. Katabi, "JMB: scaling wireless capacity with user demands," *Proceedings of the ACM SIGCOMM 2012*, pp. 235-246, August 2012.
[19] H.V. Balan, R. Rogalin, A. Michaloliakos, K. Psounis and G. Caire, "AirSync: Enabling Distributed Multiuser MIMO With Full Spatial Multiplexing,", *to appear IEEE/ACM Transactions on Networking*, vol. PP, no. 99, pp. 1, 2013
[20] D.J. Love, R. W. Heath Jr. and T. Strohmer, "Grassmannian Beamforming for Multiple-Input Multiple-Output Wireless Systems," *IEEE Transaction on Information Theory*, vol. 49, No. 10, pp. 2735-2747, October 2003.
[21] G. Golub and W. Kahan, "Calculating the singular values and pseudo-inverse of a matrix," *Journal of the Society for Industrial and Applied Mathematics, Series B*, pp. 205-224, 1965.
[22] T.M. Schmidl and D.C. Cox, "Robust Frequency and Timing Synchronization for OFDM," *IEEE Transactions on Communications*, vol. 45, no. 12, pp. 1613-1621, December, 1997.
[23] IEEE P802.11n/D2.0, "Draft STANDARD for Information Technology Telecommunications and information exchange between systems Local and metropolitan area networks Specific requirements. 20.3.11 Beamforming,".
[24] J. Zhang, M. Kountouris, J.G. Andrews and R.W. Heath Jr, "Multi-Mode Transmission for the MIMO Broadcast Channel with Imperfect Channel State Information," *IEEE Transaction on Communications*, vol. 59, no. 3,pp. 803-814, March 2011.
[25] National Instruments, "NI USRP 2921 Data Sheet," Austin, TX, 2012. [Online]. Available:http://sine.ni.com/ds/app/doc/p/id/ds-355/lang/en
[26] National Instruments, "NI LabVIEW - Improving the Productivity of Engineers and Scientists," Austin, TX, 2012. [Online]. Available:http://www.ni.com/labview/
[27] National Instruments, "GPS Disciplined Oscillator (GPSDO) Kit Data Sheet," Austin, TX, 2012. [Online]. Available:https://www.ettus.com/content/files/gpsdo-kit_4.pdf
[28] Agilent Technologies, "E4438C ESG Vector Signal Generator," [Online]. Available:http://www.home.agilent.com/en/pd-1000004297%3Aepsg%3Apro-pn-E4438C/esg-vector-signal-generator

PLACE PHOTO HERE

Seogoo Lee Biography text here.

Andreas Gerstlauer Biography text here.

Robert W. Heath Jr. Biography text here.